



ARL-TR-8769 • AUG 2019



Determination of In-Plane Shear Properties of Ultra-High-Molecular-Weight Polyethylene (UHMWPE) Composites for Input into a Thermoforming Model

by Julia Cline, Michael Yeager, and Travis Bogetti

NOTICES

Disclaimers

The findings in this report are not to be construed as an official Department of the Army position unless so designated by other authorized documents.

Citation of manufacturer's or trade names does not constitute an official endorsement or approval of the use thereof.

Destroy this report when it is no longer needed. Do not return it to the originator.



Determination of In-Plane Shear Properties of Ultra-High-Molecular-Weight Polyethylene (UHMWPE) Composites for Input into a Thermoforming Model

by Julia Cline, Michael Yeager, and Travis Bogetti

Weapons and Materials Research Directorate, CCDC Army Research Laboratory

REPORT DOCUMENTATION PAGE

Form Approved
OMB No. 0704-0188

Public reporting burden for this collection of information is estimated to average 1 hour per response, including the time for reviewing instructions, searching existing data sources, gathering and maintaining the data needed, and completing and reviewing the collection information. Send comments regarding this burden estimate or any other aspect of this collection of information, including suggestions for reducing the burden, to Department of Defense, Washington Headquarters Services, Directorate for Information Operations and Reports (0704-0188), 1215 Jefferson Davis Highway, Suite 1204, Arlington, VA 22202-4302. Respondents should be aware that notwithstanding any other provision of law, no person shall be subject to any penalty for failing to comply with a collection of information if it does not display a currently valid OMB control number.

PLEASE DO NOT RETURN YOUR FORM TO THE ABOVE ADDRESS.

1. REPORT DATE (DD-MM-YYYY) August 2019		2. REPORT TYPE Technical Report		3. DATES COVERED (From - To) 1 August 2018–02 August 2019	
4. TITLE AND SUBTITLE Determination of In-Plane Shear Properties of Ultra-High-Molecular-Weight Polyethylene (UHMWPE) Composites for Input into a Thermoforming Model				5a. CONTRACT NUMBER	
				5b. GRANT NUMBER	
				5c. PROGRAM ELEMENT NUMBER	
6. AUTHOR(S) Julia Cline, Michael Yeager, and Travis Bogetti				5d. PROJECT NUMBER	
				5e. TASK NUMBER	
				5f. WORK UNIT NUMBER	
7. PERFORMING ORGANIZATION NAME(S) AND ADDRESS(ES) CCDC Army Research Laboratory ATTN: FCDD-RLW-MB Aberdeen Proving Ground, MD 21005				8. PERFORMING ORGANIZATION REPORT NUMBER ARL-TR-8769	
9. SPONSORING/MONITORING AGENCY NAME(S) AND ADDRESS(ES)				10. SPONSOR/MONITOR'S ACRONYM(S)	
				11. SPONSOR/MONITOR'S REPORT NUMBER(S)	
12. DISTRIBUTION/AVAILABILITY STATEMENT Approved for public release; distribution is unlimited.					
13. SUPPLEMENTARY NOTES ORCID ID(s): Cline, 0000-0003-1994-3247					
4. ABSTRACT Thermoplastic composite materials can be molded into complex curvature shapes via thermoforming, where the material is heated to a pliable temperature and then formed into the desired configuration. For instance, a hemispherical composite part can be thermoformed by punching a male hemispherical tool into a flat stack of heated Ultra-High-Molecular-Weight Polyethylene (UHMWPE) composite sheets held in place by a binder ring. The quality of the as-manufactured part is dependent on many variables, including the in-plane shear constitutive response of the material, as it will dictate how easily the material conforms to the prescribed shape. Experimentally investigating the optimal set of processing parameters to achieve a hemispherical part with minimal wrinkling is time consuming and costly. Our goal is to create a computational model that can accurately simulate the thermoforming process and predict the end product quality. This will allow for rapid evaluation of optimal process parameter combinations, greatly reducing experimentation time and cost. In-plane shear characterization of DSM Dyneema HB 210 is performed at relevant process temperatures, fiber rotational rates, and preprocessing states to provide constitutive material response input for the computational process model. Biased extension tests show that an elevated temperature leads to an increase of the in-plane shear compliance. Rate effects are more pronounced at a lower temperature. Fiber rotation is upwards of $\pm 35^\circ$ for all specimens. LS-DYNA finite element simulations, using select in-plane shear response inputs, demonstrate the effect of the in-plane shear response on the thermoforming process, the as-manufactured part thickness, and in-plane shear distributions.					
15. SUBJECT TERMS UHMWPE, in-plane shear characterization, process modeling, bias extension testing, LS-DYNA simulations					
16. SECURITY CLASSIFICATION OF:			17. LIMITATION OF ABSTRACT UU	18. NUMBER OF PAGES 26	19a. NAME OF RESPONSIBLE PERSON Julia Cline
a. REPORT Unclassified	b. ABSTRACT Unclassified	c. THIS PAGE Unclassified			19b. TELEPHONE NUMBER (Include area code) 410-306-1949

Contents

List of Figures	iv
List of Tables	iv
Acknowledgments	v
1. Introduction	1
2. Methodology and Approach	2
3. Experimental Design and Analysis	3
3.1 Specimen Preparation	3
3.2 Experimental Setup	4
3.3 Analysis Approach	5
3.4 Computational Model	6
3.5 Boundary Conditions	7
3.6 Material and Element Information	7
4. Results	8
4.1 In-plane Shear Characterization	8
4.2 Computational Process Model	12
5. Conclusions	14
6. References	16
Distribution List	19

List of Figures

Fig. 1	An overview of the thermoforming process, where a flat stack of material is heated prior to being (a) secured in a binder ring and (b) thermoformed into a hemispherical shape	1
Fig. 2	The experimental setup for the testing of the quasi-static bias extension specimens showing the full load train, stereovision DIC setup. The environmental chamber, denoted by the dashed line, surrounds the grips and specimen.....	4
Fig. 3	Stress–strain curve for the HB210 specimens tested in open air and through the environmental chamber window	5
Fig. 4	A sketch denoting the undeformed \vec{A} and \vec{B} and deformed \vec{a} and \vec{b} fiber positions, the fiber angle θ , and the engineering shear strain γ ...	6
Fig. 5	(a) Exploded view of the thermoforming model, outlining key parts, and (b) the initial and final configuration of the thermoforming model.....	7
Fig. 6	Engineering stress–shear strain curves to evaluate rate dependency of unconsolidated specimens tested at (a) 25 °C, (b) 100 °C, and (c) 130 °C	8
Fig. 7	Engineering stress–shear strain to evaluate rate dependency of consolidated specimens tested at (a) 25 °C, (b) 100 °C, and (c) 130 °C	9
Fig. 8	Engineering stress–shear strain curves to evaluate temperature dependency of unconsolidated specimens tested at (a) 0.1 °/s, (b) 0.7 °/s, and (c) 7 °/s.....	10
Fig. 9	Engineering stress–shear strain curves to evaluate temperature dependency of consolidated specimens tested at (a) 0.1 °/s, (b) 0.7 °/s, and (c) 7 °/s.....	10
Fig. 10	A comparison of unconsolidated and consolidated average response at 0.7 °/s as a function of temperature	11
Fig. 11	Correlation between trilinear fit and characterized shear constitutive response for a shear rate of 0.7°/s.....	12
Fig. 12	Predictions for shear distribution and wrinkle formation in unconsolidated sheets of UHMWPE	13
Fig. 13	Predictions for shear distribution and wrinkle formation in consolidated sheets of UHMWPE	13

List of Tables

Table 1	Maximum fiber rotation values measured for all configurations tested	11
---------	--	----

Acknowledgments

The authors acknowledge Jim Wolbert, Mike Neblett, and Freddie Racine (US Army Combat Capabilities Development Command Army Research Laboratory) for panel manufacturing and specimen preparation. Additionally, the work of Dr Tim Walter, Dave Gray, and Paul Moy in installing and setting up the environmental chamber is gratefully acknowledged.

1. Introduction

Ultra-High-Molecular-Weight Polyethylene (UHMWPE) composite materials are widely used in soft body armor and helmets because they are lightweight and they exhibit superior ballistic performance.¹⁻³ These materials are typically supplied from the manufacturer in cross-ply rolls and are cut into flat sheets prior to manufacturing parts. Significant research continues today into manufacturing methods that take flat material sheets and form them into complex curved shapes, without introducing manufacturing defects like wrinkles and overlaps.⁴⁻⁸ Wrinkles are a common manufacturing defect that affect ballistic performance by blocking the energy dissipation paths. The transverse waves are reflected at each wrinkle and reduce energy absorption, which reduces protective capabilities. Both the wavelength and amplitude of wrinkles are detrimental to the ballistic performance.⁹ Some experimental “cut and dart” methods of strategically placing cuts into the flat sheets are used to reduce defects⁶; however, cutting fibers can be detrimental to the fiber strength (which impacts ballistic performance) and introduces seams into the shape.⁵ More sophisticated thermoforming techniques have been used to preform UHMWPE materials into the desired shape prior to consolidation under heated compaction.⁷ For instance, a hemispherical composite part can be thermoformed by punching a male hemispherical tool into a flat stack of heated UHMWPE composite sheets held in place by a binder ring (see Fig. 1). This process has been shown to significantly reduce defects in the final part.^{8,10}

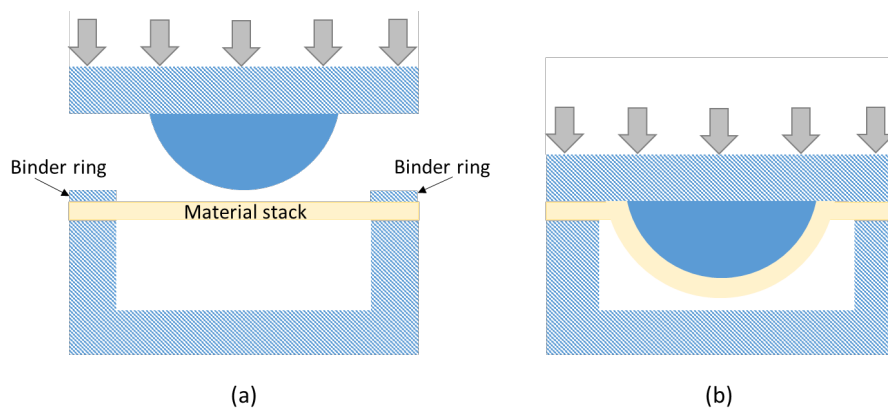


Fig. 1 An overview of the thermoforming process, where a flat stack of material is heated prior to being (a) secured in a binder ring and (b) thermoformed into a hemispherical shape

The quality of the final thermoformed part is dependent on many variables including the punch rate, friction between the composite and tooling, binder ring pressure, and the material properties.^{4,8,10-12} Achieving a hemispherical shape with minimal wrinkling is the desired outcome. However, experimentally investigating the optimal set of processing parameters to achieve this outcome is time consuming

and costly. Computational models that accurately simulate the thermoforming process and predict the as-manufactured part quality have the potential to significantly reduce experimentation time and cost by rapidly evaluating process parameter combinations and recommending an optimal set.

Past research has been focused on developing these types of predictive models for woven composites^{4,13,14} and fewer models exist for cross-ply thermoplastic composites.^{8,10,15,16} To ensure accurate and realistic predictions, the simulations rely on input parameters that accurately describe the material constitutive response under conditions (i.e., temperatures and loading rates) experienced during the thermoforming process.

2. Methodology and Approach

The in-plane shear response of the composite is a critical input for the numerical model, as it will dictate how easily the material conforms to the prescribed shape.¹⁷ It has been demonstrated that UHMWPE composite materials undergo significant fiber rotation when loaded in shear, due to the nature of stiff, strong fibers being embedded in a very compliant matrix.¹⁸ This is the primary material deformation mechanism during thermoforming. It is therefore important to understand the in-plane shear constitutive behavior of these materials at temperatures and strain rates relevant to the thermoforming process.

There are two main test methods that have been used to characterize in-plane shear behavior: the picture frame test and the bias extension test.¹⁹⁻²¹ Each has its own pros and cons. The picture frame test has been shown to be more representative of the material deformation that occurs during preforming than the bias extension test for woven materials; Harrison et al.¹⁹ recommend that the two methods can be used in conjunction to characterize a material. A comparative study for cross-ply UHMWPE materials does not exist. The picture frame test requires a relatively elaborate experimental setup and specimen design. Picture frame tests must be performed at elevated temperature²⁰ as the material is much stiffer at room temperature. The bias extension test (ASTM D3516²¹) is based on a simple rectangular specimen in a tensile loading configuration with the fiber directions oriented at $\pm 45^\circ$ to the loading direction. This test method has been shown to achieve sufficient shear deformation at room temperatures for UHMWPE composites¹⁸ and can be performed at elevated temperatures as well. Recently, we demonstrated that material relationships generated using the bias extension test can be used to accurately simulate the results of the picture frame test.¹⁶ Consequently, in this work, we focus on characterizing the UHMWPE composite material constitutive response using the bias extension test. The in-plane shear material

response is input into a finite-element-based thermoforming process model to predict wrinkle formation, shear strain, and thickness distributions during thermoforming. The process model is used to study the influence of various process parameters, temperature, and strain rate on model predictions.

3. Experimental Design and Analysis

A common ballistic thermoplastic composite is chosen for this work, DSM Dyneema's hard ballistic HB210, which is high-strength SK-99 UHMWPE fibers embedded in a polyurethane matrix.³ We evaluate the effects of temperature, loading rate, and consolidation on the in-plane shear response of the material. Characterization is performed at temperatures relevant to material forming from room temperature (25 °C) to the recommended consolidation temperature (130 °C). Temperatures above 130 °C are not explored, as we do not want to melt the material. The process model is preliminarily used to identify local shear rates that are relevant during forming. These rates are determined from simulations that incorporate typically used punch cross-head displacement rates. The effect of consolidation is evaluated by testing $[0/90]_2$ sheets of material taken directly off the roll and comparing the response to the material after consolidation using a hot-press.

3.1 Specimen Preparation

DSM Dyneema HB210 is commercially available on a continuous roll of sheet material consisting of four plies in a $[0/90]_2$ configuration. Specimens for testing are cut from a single sheet using a Gerber cutting table into 15.2-cm-long by 2.5-cm-wide rectangles such that the fibers are oriented at $\pm 45^\circ$ to the length of the specimen. The average thickness for the specimen is 0.196 mm. Additional "consolidated" specimens are waterjet cut from sheet material that has been consolidated under a hot press at 20.7 MPa and 132 °C for 60 min in a confined aluminum mold with active heating and cooling. The average thickness of the consolidated specimens is 0.179 mm. A speckle pattern is applied to the specimen surface using Rust-oleum Industrial Choice spray paint so that digital image correlation (DIC) can be used to track surface deformation. First, a thin layer of flat white spray paint is applied to the surface and allowed to dry. Black speckles are added by lightly spraying the paint over the specimens and allowing droplets to fall randomly on the specimen surface. Finally, a layer of Krylon dulling spray is applied to the surface to reduce reflections off the specimen surface during testing. This painting procedure produces a trackable speckle pattern that remains adhered to the specimen surfaces at elevated temperatures.

3.2 Experimental Setup

Tensile tests are performed on an Instron Model 4206 screw-driven electromechanical test frame with a 2500-N load cell and lightly serrated wedge action grips. An Instron environmental chamber with a viewing window is installed on the frame to enable elevated temperature testing. The environmental chamber temperature and readings from a type-K thermocouple in contact with the grips are used to determine when the chamber is at the desired temperature. A noncontact infrared thermometer is also used to measure the specimen surface temperature prior to testing.

DIC is used for deformation measurement. Two 2.3-MPixel Point Grey cameras with 105-mm micro-Nikkor lenses are positioned in a stereovision configuration (Fig. 2) to look through the viewing window. VIC Snap software²² is used to capture images throughout the loading cycle. The cameras are oriented vertically, such that the long axis is parallel to the specimen length. Voltage output from the test frame, corresponding to load and crosshead displacement, is connected to the DIC computer. The voltage output is converted by the VIC Snap software using a scale factor and recorded for each image taken.

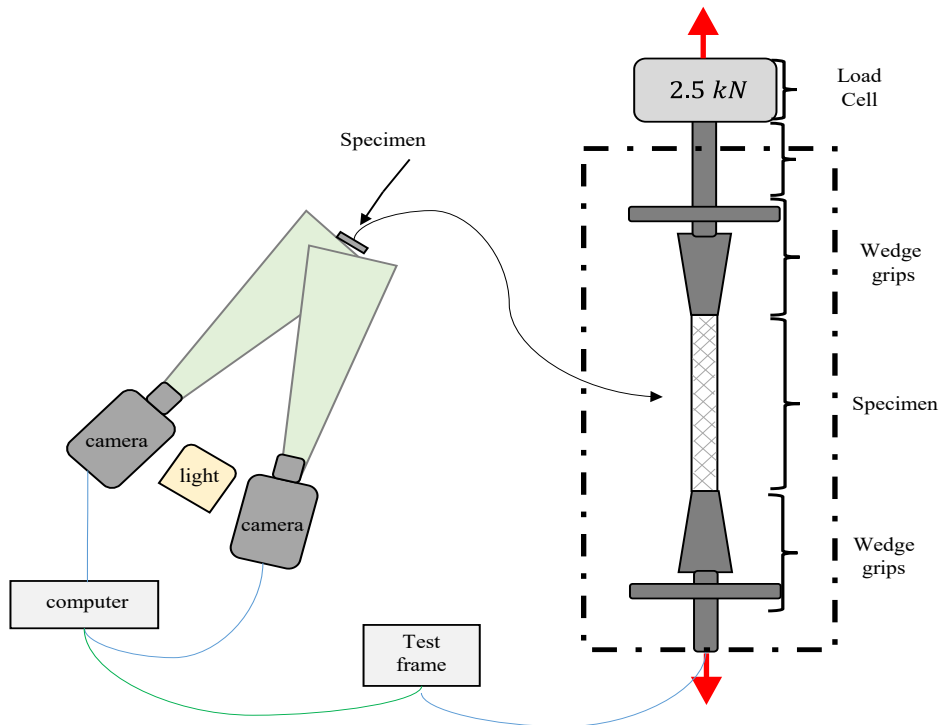


Fig. 2 The experimental setup for the testing of the quasi-static bias extension specimens showing the full load train, stereovision DIC setup. The environmental chamber, denoted by the dashed line, surrounds the grips and specimen.

Tests are run in displacement control until ultimate failure at rates of 6.35 mm/min, 36 mm/min, and 360 mm/min, which correspond to shear strain rates of interest in the thermoforming model of 0.1 °/s, 0.7 °/s, and 7 °/s, respectively. Specimens fail in delamination in the gage section.

3.3 Analysis Approach

DIC images for each specimen test are imported into the VIC3D²² correlation software and processed using incremental correlation, whereby the correlation compares the current image to the previous one rather than the original undeformed reference image. This approach ensures that the large deformation is captured accurately. To confirm that the environmental chamber window is not influencing the deformation measurements, room temperature tests performed in open air and through the chamber window are compared in Fig. 3. By following the recommendations from Correlated Solutions²³ and adjusting the distortion correction in the calibration step, similar results are observed for each configuration. The average Green–Lagrange strains in the loading direction (E_1) and the transverse direction (E_2) for each specimen are exported for data postprocessing analysis, along with the corresponding load histories.

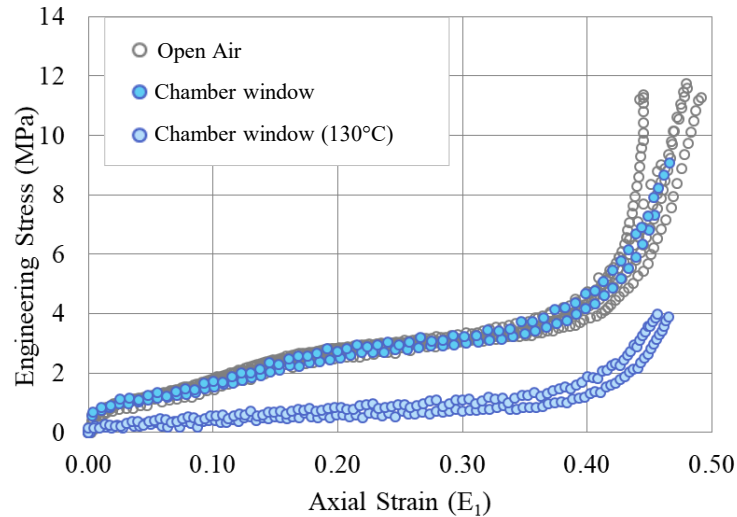


Fig. 3 Stress–strain curve for the HB210 specimens tested in open air and through the environmental chamber window

It is well known that for a specimen with a $\pm 45^\circ$ layup tested in tension that the fibers will rotate toward the direction of loading,^{18,21,24} commonly referred to as fiber scissoring²⁴ or reorientation. It is clear that the fibers in the HB210 material are rotating by the significant stiffening behavior observed just prior to ultimate failure (see Fig. 3). To accurately characterize the in-plane shear response of the HB210

composite, we employ a finite deformation–based approach, outlined in Cline et al.,¹⁸ to quantify the fiber rotation and understand its effect on the material behavior.

Referring to Fig. 4, the angle between the fibers \vec{A} and \vec{B} is defined as $\pm\theta$ where $\theta = 45^\circ$ initially and decreases as load is applied. The deformed fibers are denoted by vectors, \vec{a} and \vec{b} . We define the deformation in the loading direction (1) and transverse direction (2) as stretches λ and α , respectively. Deformation in the thickness (3) direction is not considered in this analysis. The stretches are calculated from the Green–Lagrange strains and are used to calculate the angle ($\pm\theta$) between the fibers at each load step. Accordingly, the engineering shear strain is defined as $\gamma = 90^\circ - 2\theta$.

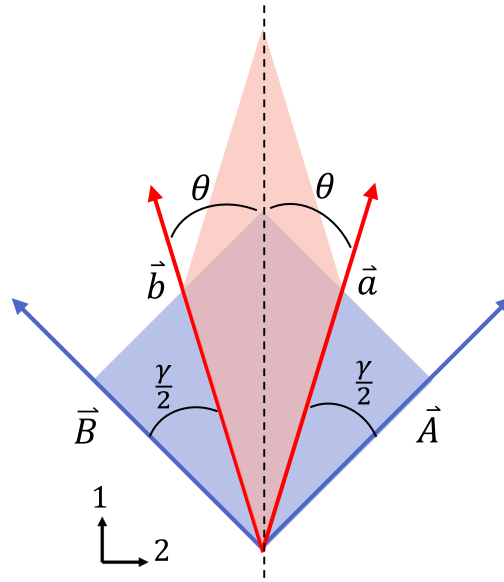


Fig. 4 A sketch denoting the undeformed \vec{A} and \vec{B} and deformed \vec{a} and \vec{b} fiber positions, the fiber angle θ , and the engineering shear strain γ

3.4 Computational Model

A finite element-based model is developed in LS-DYNA to predict the mechanical deformation of UHMWPE sheets during the thermoforming process. The explicit dynamics solid mechanics model, shown in Fig. 5a, includes a punch, binder plate, die plate, and a single sheet of the UHMWPE material. The punch deforms the material by pushing it through the die plate, while the binder provides an out-of-plane force to resist material wrinkling. Through friction, the binder also supplies an in-plane constraint on the UHMWPE material, inducing in-plane shear deformation. The simulation is completed once the punch is fully embedded in the UHMWPE material.

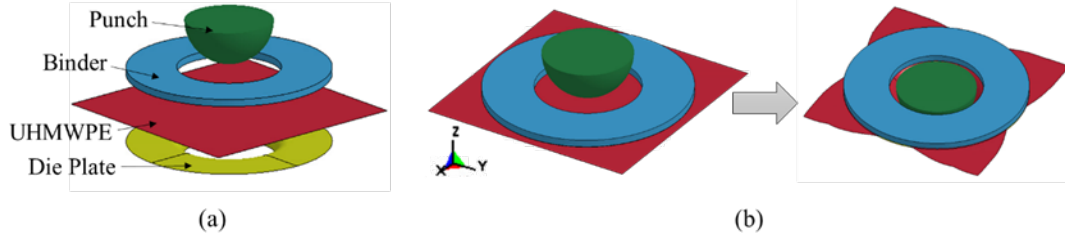


Fig. 5 (a) Exploded view of the thermoforming model, outlining key parts, and (b) the initial and final configuration of the thermoforming model

3.5 Boundary Conditions

Initially, the binder and die plate begin contacting the flat sheet of UHMWPE material, with the punch offset by 1 mm. The punch has a fixed velocity boundary condition applied to the nodes on its top surface. The location of the die plate is fixed in all directions because it is anchored during the process. The binder plate has an applied vertical (z-direction) load and is constrained to only permit vertical motion. The vertical load corresponds to an applied pressure of 6.5 kPa, which has been used in literature for UHMWPE thermoforming.¹⁶ The static and dynamic friction coefficients between the tooling and UHMWPE were set to 0.08 and 0.07, respectively. The initial and final states of the model are shown schematically in Figure 5b.

3.6 Material and Element Information

This model uses built-in LS-DYNA material and element formulations. A rigid material definition is used to define the tooling (binder, die plate, punch). The UHMWPE material is represented with a fabric material model, which allows the shear stress–strain relationship to be described using a trilinear curve. The accuracy of the least squares trilinear fit will be evaluated in the Results section. The material does not include rate-dependent properties (the validity of which will be addressed in the Results section). The UHMWPE material sheet, with a $[0/90]_2$ architecture, is assumed to have identical in-plane orthogonal stiffnesses, E_x and E_y , which are set to 22 GPa for all trials (the model is not sensitive to small changes in fiber direction modulus). The model uses 16,129 fully integrated shell elements (Type 16 in LS-DYNA) to model the UHMWPE material sheet. Changing the element size to include 36,100 elements in the UHMWPE sheet had no noticeable influence on the shear strain field, thus it can be said that the model is converged.

4. Results

4.1 In-plane Shear Characterization

Strains are averaged over the gage section; the average engineering shear stress–shear strain curves for the HB210 specimens are shown in Fig. 6 as a function of test temperature. Rate dependence is most prominent during room temperature tests (25 °C) where the stiffness and strength of the material increases with increasing rate. At elevated temperatures, there is only a slight increase of failure strength with increasing rate, indicating that the rate effect is substantially less for higher temperatures.

For the consolidated specimens, rate differences at room temperature (Fig. 7a) between 0.1 °/s and 0.7 °/s are not as substantial as for the unconsolidated specimens (Fig. 6a).

Similar to the unconsolidated specimens, rate does not play a significant role in the material response at elevated temperature (see Figs. 7b and 7c).

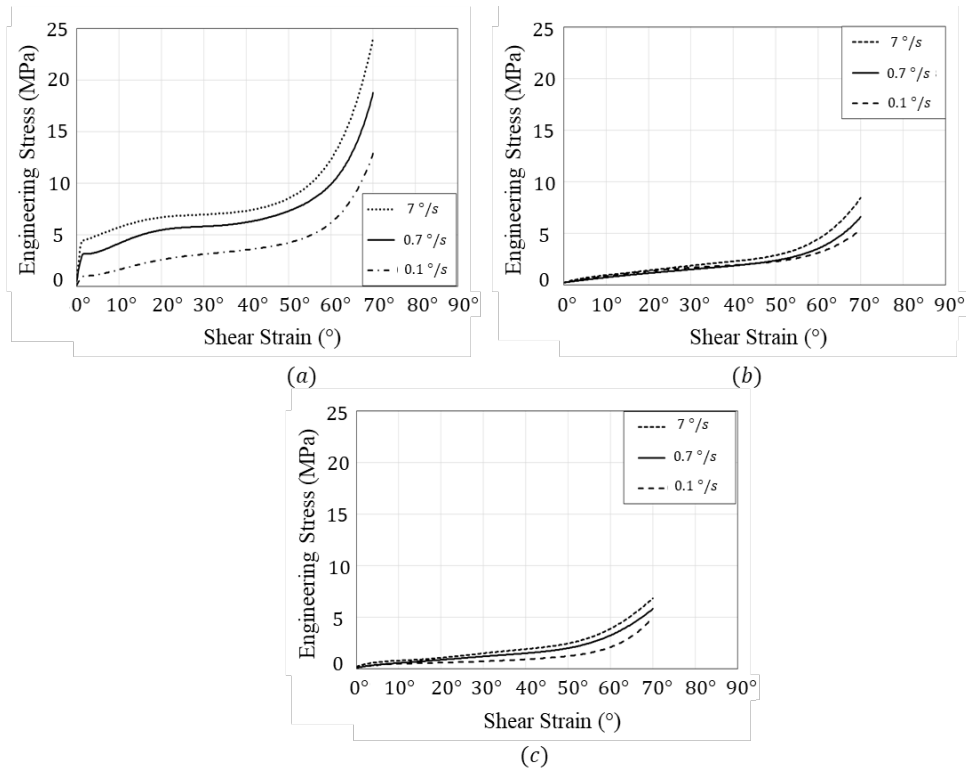


Fig. 6 Engineering stress–shear strain curves to evaluate rate dependency of unconsolidated specimens tested at (a) 25 °C, (b) 100 °C, and (c) 130 °C

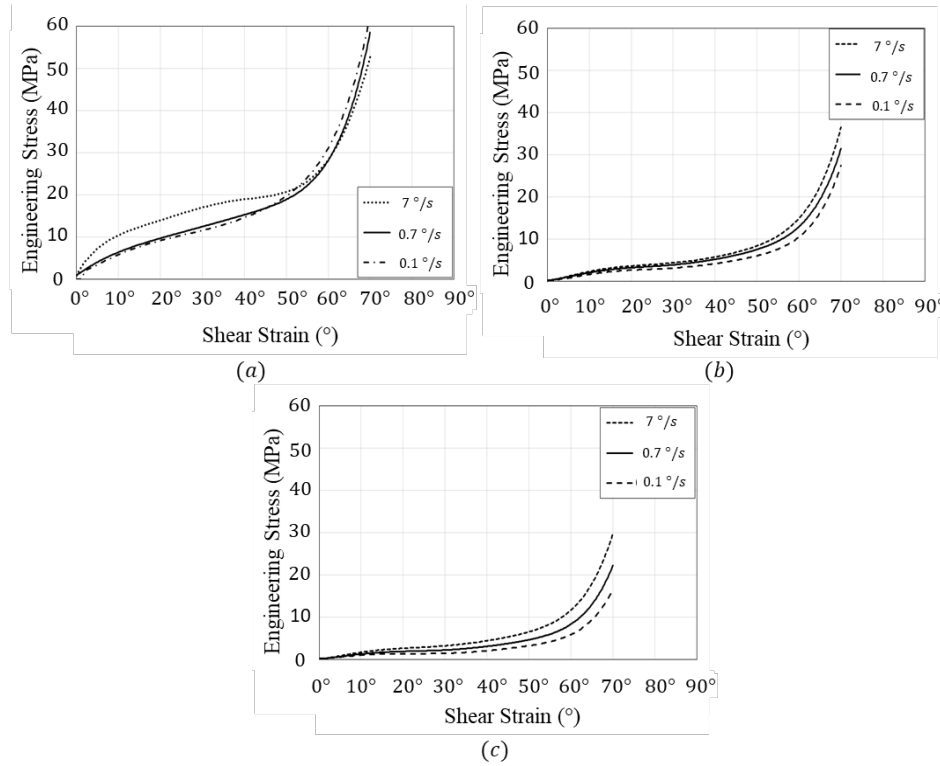


Fig. 7 Engineering stress–shear strain to evaluate rate dependency of consolidated specimens tested at (a) 25 °C, (b) 100 °C, and (c) 130 °C

Temperature also has an effect on the shear properties of the HB210 material. Figures 8a–8c show that for each rate tested, as temperature is increased, the material becomes more compliant. This effect is most pronounced in the 7 °/s with nearly a 64% drop in failure stress between the room temperature (25 °C) and 100 °C specimens. Little difference between tests at 100 °C and 130 °C indicates that the material has softened as much as it will before melting. Additional tests were run at intermediate temperatures at 0.7 °/s to understand when maximum softening is reached. The softening is found to be progressive with increasing temperatures (Fig. 8b).

Similar trends hold true for the consolidated material. The material compliance reduces significantly with increasing temperature, as shown in Fig. 9. Very little difference between rates 0.1 °/s and 0.7 °/s is observed at all temperatures.

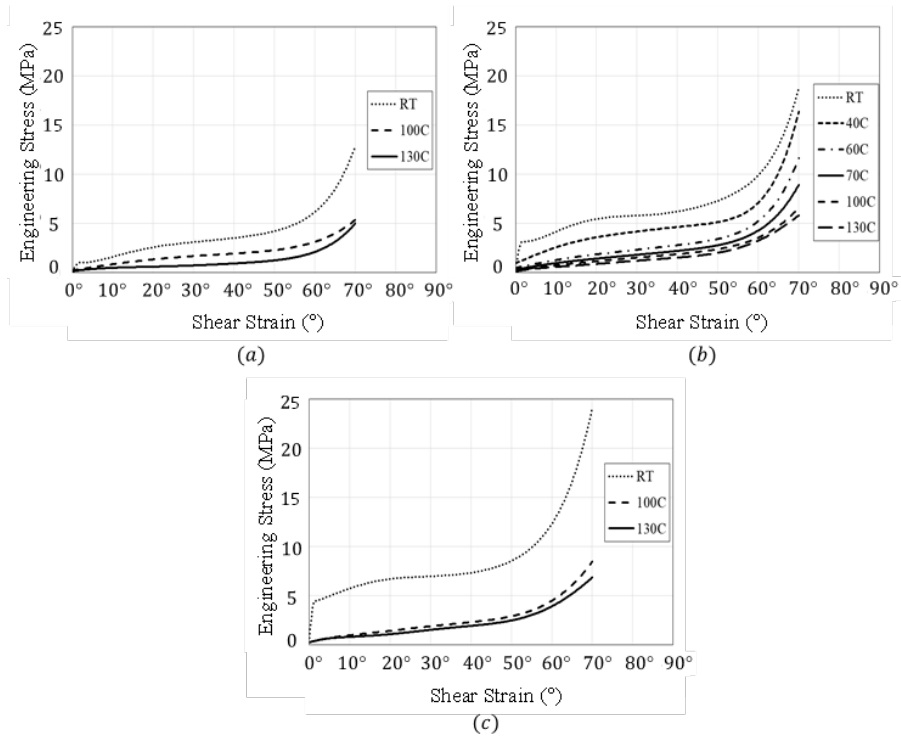


Fig. 8 Engineering stress–shear strain curves to evaluate temperature dependency of unconsolidated specimens tested at (a) 0.1 °/s, (b) 0.7 °/s, and (c) 7 °/s

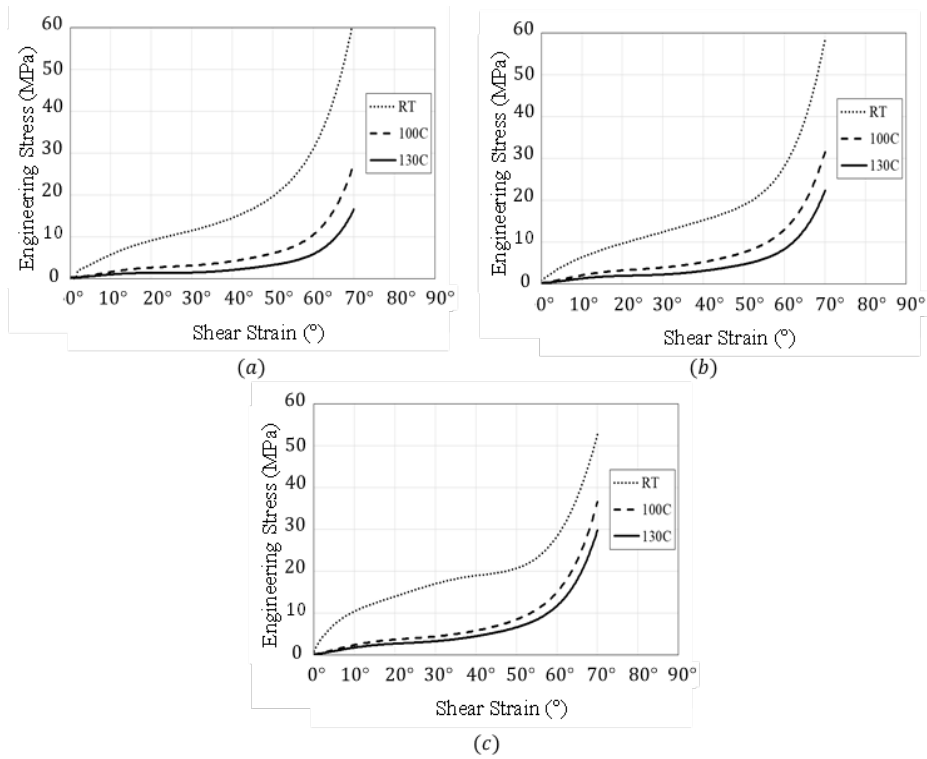


Fig. 9 Engineering stress–shear strain curves to evaluate temperature dependency of consolidated specimens tested at (a) 0.1 °/s, (b) 0.7 °/s, and (c) 7 °/s

Figure 10 presents a comparison of the average in-plane shear behavior for the unconsolidated and consolidated specimens tested at 0.7 °/s. From this comparison, we can see that consolidation affects the strength and stiffness of the material. It does not affect the maximum shear strain, however. The maximum shear strain (at failure) is to be independent of whether the material was consolidated or not and independent of the rate and temperature it was tested. This maximum was found to be $69.5^\circ \pm 1.6^\circ$, as shown in Table 1.

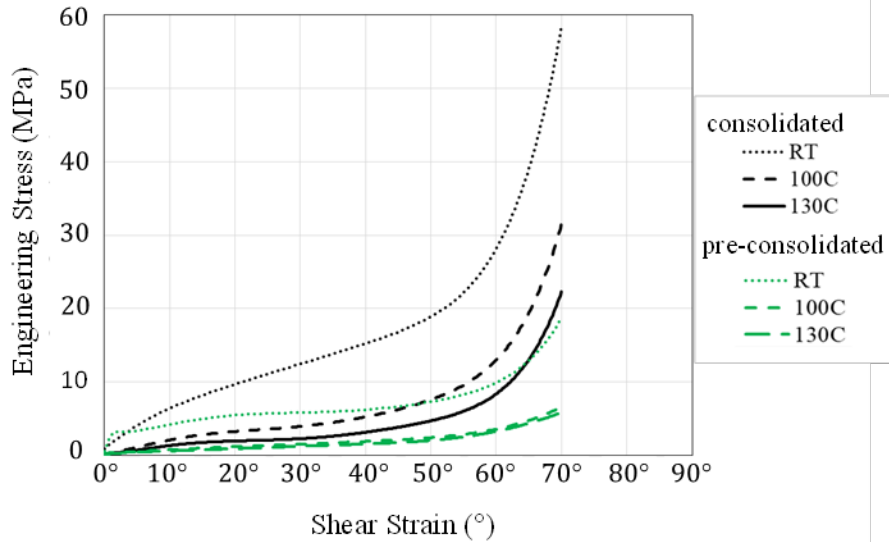


Fig. 10 A comparison of unconsolidated and consolidated average response at 0.7 °/s as a function of temperature

Table 1 Maximum fiber rotation values measured for all configurations tested

Configuration	Temperature\Rate	0.1 °/s	0.7 °/s	7 °/s
(a) Unconsolidated	25°C	67.7°	70.8°	69.2°
	40°C	...	68.4°	...
	60°C	...	69.1°	...
	70°C	...	68.3°	...
	100°C	70.6°	70.6°	70.6°
	130°C	67.9°	69.1°	68.1°
(b) Consolidated	25°C	69.5°	70.3°	70.2°
	100°C	64.4°	69.9°	69.7°
	130°C	70.9°	71.5°	71.7°

4.2 Computational Process Model

As mentioned previously, the thermoforming process model uses a trilinear fit to describe the shear stress–strain response of the UHMWPE material. The trilinear input is shown with the experimentally characterized shear behavior for a rate of $0.7 \text{ }^\circ/\text{s}$ in Fig. 11.²⁵ The close match with the experimental data for the unconsolidated sheets shows that the response can be accurately represented by a trilinear fit, a trend that held for all loading rates and the consolidated sheets. It is noted that there was a very large change in shear modulus when changing from room temperature to $100 \text{ }^\circ\text{C}$, but only a small change between $100 \text{ }^\circ\text{C}$ and $130 \text{ }^\circ\text{C}$.

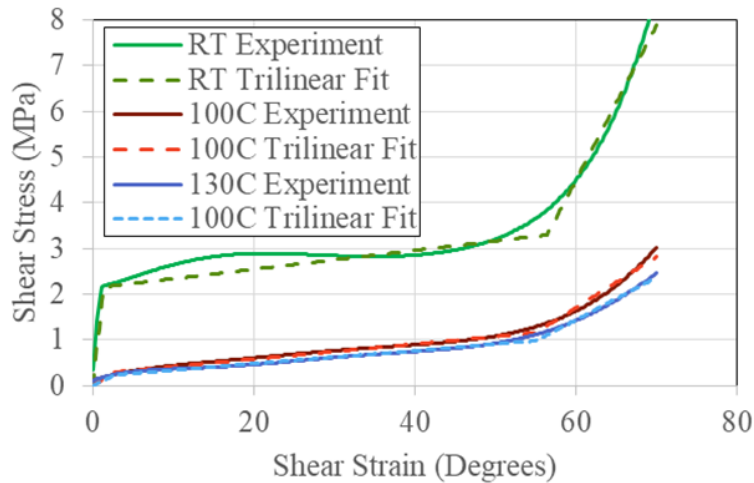


Fig. 11 Correlation between trilinear fit and characterized shear constitutive response for a shear rate of $0.7^\circ/\text{s}$

When the punch is fully embedded in the UHMWPE sheet, the simulations are complete. The deformation state at this time for the unconsolidated sheets over a range of shear rates and temperatures is shown in Fig. 12. Again, when shear rate is referenced, it is in the context of the rate used to characterize the input shear response. The in-plane shear distribution within the UHMWPE sheet is shown for the areas that will comprise the final hemisphere part. The thickness change is directly related to the in-plane shear deformation through conservation of volume.⁸ For context, a shear angle of 59° corresponds to a thickness increase of about 100% when compared to a 0° shear angle. The wrinkles forming in and around the part are also shown over the range of rates and temperatures. Large wrinkle formation is found for the room temperature simulations using the higher shear rate properties. Wrinkles form for the $0.1 \text{ }^\circ/\text{s}$ shear response but are much smaller than those in the $0.7 \text{ }^\circ/\text{s}$ and $7 \text{ }^\circ/\text{s}$ cases. As a result of the large wrinkles, the material is not forced to undergo as much shear deformation. For the consolidated sheets, shown in Fig. 13, large wrinkles form at room temperature for all the loading rates due to the large shear stiffness (shown in Fig. 10).

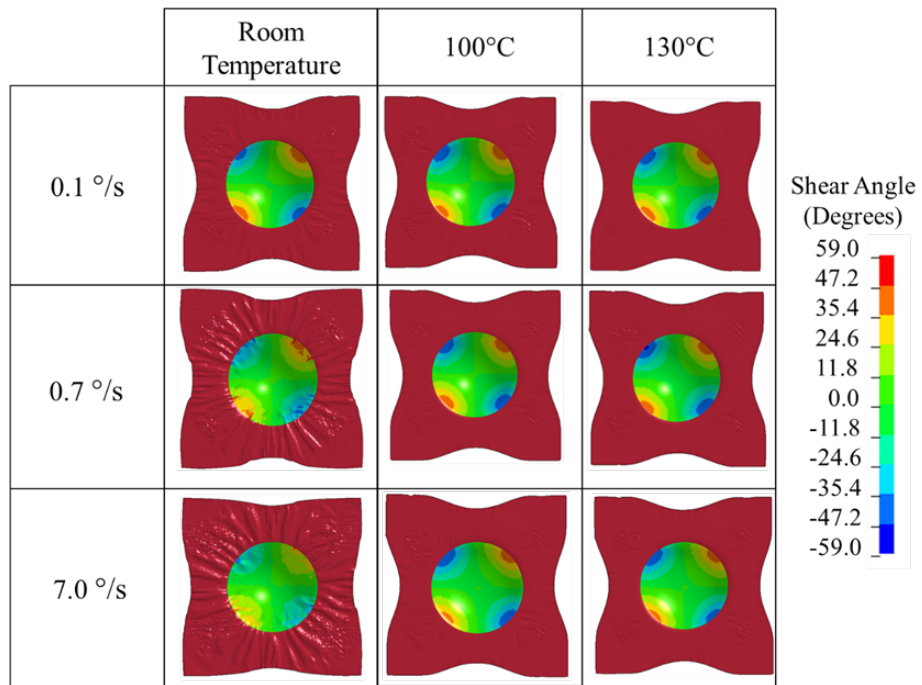


Fig. 12 Predictions for shear distribution and wrinkle formation in unconsolidated sheets of UHMWPE

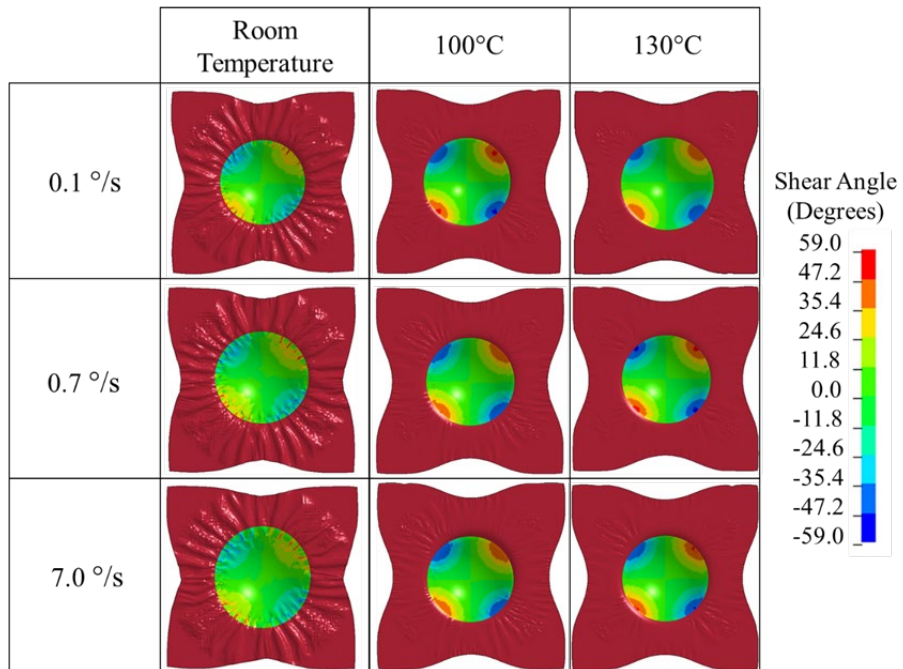


Fig. 13 Predictions for shear distribution and wrinkle formation in consolidated sheets of UHMWPE

At elevated temperatures (at which thermoforming is performed), the rate effects on both unconsolidated and consolidated sheet forming are negligible for both wrinkle development and shear deformation (and in turn thickness gradients). This validates the assumption that the thermoforming process can be modeled quasi-statically (no rate-dependent shear properties required).

The predictions for the unconsolidated sheets using the 100 °C and 130 °C properties are almost identical, which is expected since the shear response does not change much between those temperatures. As seen in Fig. 13, the temperature increase is not predicted to have a significant role in forming the consolidated sheets, but there are some small wrinkles in the 100 °C cases that are not present at the 130 °C cases. These results suggest that from the options shown, thermoforming of unconsolidated sheets should be done at 100 °C to save time and heating costs without compromising part quality. At this temperature, the higher rates are preferable to further optimize process time since there is minimal difference between 0.1 °/s and 7 °/s.

5. Conclusions

Thermoplastic composite materials are typically preformed from unconsolidated sheets in loose stacks. This work sought to evaluate the effect of temperature, rate, and preprocessing configuration on the in-plane shear behavior of HB210 UHMWPE fiber composite material that is commonly used in ballistic helmets. This characterization effort is important as in-plane shear deformation is the primary deformation mechanism during preforming as the material must shear to conform to a double curvature shape. Computational simulations show the effect of the shear properties on the predicted preformed part.

Characterization of HB210 is conducted at temperatures (25 °C, 100 °C, and 130 °C) and rates (0.1 °/s, 0.7 °/s, and 7 °/s) that are relevant to the preforming process. The effect of preprocessing configuration is also evaluated by testing specimens that are cut from both unconsolidated off-the-roll sheets and consolidated sheets.

This investigation shows that the rotation rate has the most effect at room temperature for both the preconsolidated and consolidated material. Rate increases the stiffness and strength of the material, but this effect is less pronounced at elevated temperature. Temperature is shown to reduce the stiffness and strength of the material as it is increased. Shear compliance does not increase substantially at temperatures above 100 °C. Several intermediate temperatures (40 °C, 60 °C, and 70 °C) are tested for preconsolidated HB 210 at a rotation rate of 0.7 °/s to determine the progressive reduction in shear compliance. In comparing the

preconsolidated material response with the consolidated material at the same rate as a function of temperature, we can see that the strength and stiffness of the material are affected by the consolidation process but the deformation is not. Rotations on average of $\pm 35^\circ$ are observed for specimens in all test configurations.

The in-plane shear relationships are used in a computational model to assess the influence of the input shear response on wrinkle formation and shear distribution in preformed hemispheres. It is shown that the shear rate significantly influences the deformation mechanisms at room temperature but does not play a role at elevated temperatures (over the range studied), which validates the choice of a rate-independent processing model. Furthermore, the model predicts that there is no added benefit from increasing the temperature from 100 °C to 130 °C, leading to the recommendation that the lower temperature be used in the process. Of the configurations tested, the model predicted the largest wrinkle formation if a room temperature stack of preconsolidated material preformed quickly (7 °/s). Wrinkling is reduced significantly at elevated temperatures.

Based on this work we can identify suggested process temperatures and rates for thermoforming UHMWPE hemispheres without significant wrinkling in the final part. The computational model predictions will be verified in the future by comparing with experimentally preformed hemispheres.

6. References

1. Karthikeyan K, Russell B, Fleck N, Wadley H, Deshpande V. The effect of shear strength on the ballistic response of laminated composite plates. *Eur J Mech A-Solid*. 2013;42:35–53.
2. Russell B, Karthikeyan K, Deshpande V, Fleck N. The high strain rate response of ultra high molecular-weight polyethylene: from fibre to laminate. *Int J Impact Eng*. 2013;60:1–9.
3. DSM Dyneema Industries [accessed 2019 Apr]. http://www.dsm.com/products/dyneema/en_US/home.html.
4. De Luca P, Pickett A, Queckborner T, Johnson A. Development validation and first industrial numerical results of a finite element code to simulate the thermoforming process. 4th International Conference on Automated Composites (ICAC'95); 1995; Nottingham, UK.
5. Hallender P, Akermo M, Mattei C, Petersson M, Nyman T. An experimental study of mechanisms behind wrinkle development during forming of composite laminates. *Compos Part A*. 2013;50:54–64.
6. Cunniff P, Parker J. The effect of preform shape on ballistic impact performance, coverage and seam density on combat helmets. *Proceedings of 24th International Symposium on Ballistics*; 2007; New Orleans, LA.
7. Cartwright B, Mulcahy N, Chhor A, Thomas S, Suryanarayana M, Sandlin J, Crouch I, Naebe M. Thermoforming and structural analysis of combat helmets. *J Manufacturing Sci Eng*. 2015;137:1–9.
8. Dangora L, Mitchell C, Sherwood J, Parker J. Deep-drawing forming trials on a cross-ply thermoplastic lamina for helmet preform manufacture. *J Manuf Sci E*. 2017;139:1–8.
9. Parker J, Cyganik J, Kayhart T, Kubiak D, Sykes R. The effect of out-of-plane fiber waviness on the ballistic performance of ultra high molecular weight polyethylene (UHMWPE) laminates. *29th International Symposium on Ballistics*; 2016; Edinburgh, Scotland.
10. Ahn H, Kuuttila N, Pourboghrat F. Thermo-hydroforming of a fiber-reinforced thermoplastic composites considering fiber orientations. *Proceedings of the 21st International ESAFORM Conference on Material Forming*; 2018; Palermo, Italy.

11. Ersoy N, Potter K, Wisnom M, Clegg M. An experimental method to study the frictional processes during composites manufacturing. *Compos Part A*. 2005;36:1536–1544.
12. Fetfatsidis K, Gamache L, Gorczyca J, Sherwood J. Design of an apparatus for measuring tool/fabric and fabric/fabric friction of woven-fabric composites during the thermostamping process. *Int J Mater Form*. 2011;6(1):1–11.
13. Pickett A, Queckborner T, De Luca P, Haug E. An explicit finite element solution for the forming prediction of continuous fibre-reinforced thermoplastic sheets. *Compos Manuf*. 1995;6:237–243.
14. Johnson A, Pickett A. Numerical simulation of forming process in long fibre reinforced thermoplastics. *Composites Material Technology V, Transactions on Engineering Sciences*. 1996;10.
15. Dangora L, Mitchell C, White K, Sherwood J, Parker J. Characterization of temperature-dependent tensile and flexural rigidities of a cross-ply thermoplastic lamina with implementation into a forming model. *Int J Mat Form*. 2018;1(11):43–52.
16. White K, Yeager M, Sherwood J, Bogetti T, Cline J. Material characterization and finite element modeling for the forming of highly oriented UHMWPE thin-film and unidirectional cross-ply composites. *Proceedings of the 33rd ASC Technical Conference*; 2018; Seattle, WA.
17. White K, Sherwood J. Finite element simulation of thickness changes in laminate during thermoforming. *Proceedings of the 20th International ESAFORM Conference on Material Forming*; 2018; Palermo, Italy.
18. Cline J, Bogetti T, Love B. Comparison of the in-plane shear behavior of UHMWPE fiber and highly oriented film composites. *Proceedings of the 32nd ASC Technical Conference*; 2017; West Lafayette, IN.
19. Harrison P, Clifford M, Long A. Shear characterization of viscous woven textile composites: a comparison between picture frame and bias extension experiments. *Compos Sci Tech*. 2004;64:1453–1465.
20. Dangora L, Hansen C, Mitchell C, Sherwood J, Parker J. Challenges associated with shear characterization of cross-ply lamina using picture frame tests. *Compos Part A*. 2015;78:181–190.
21. D3518/D3518M-13. Standard test method for in-plane shear response of polymer matrix composite materials by tensile test of a $\pm 45^\circ$ laminate. West Conshohocken (PA): ASTM International; 2016.

22. Correlated Solutions, Inc. [accessed 2019 Apr]. <http://www.correlatedsolutions.com>.
23. Simonsen M, Byrne E. Viewing through a window. Correlated Solutions, Inc. [accessed 2019 Apr]. <https://www.correlatedsolutions.com/support/index.php?Knowledgebase/Article/View/49/1/viewing-through-a-window>.
24. Sun CT, Zhu C. The effect of deformation induced change of fiber orientation on the non-linear behavior of polymeric composite laminates. *Compos Sci Technol*. 2000;60:2337–2345.
25. Yeager M, Cline J, White K, Bogetti T, Sherwood J. A methodology for characterization and modeling in-plane shear deformation in UHMWPE composites. Aberdeen Proving Ground (MD): Army Combat Capabilities Development Command Army Research Laboratory (US); 2019. ARL Technical Report in preparation.

1 DEFENSE TECHNICAL
(PDF) INFORMATION CTR
DTIC OCA

1 CCDC ARL
(PDF) FCDD RLD CL
TECH LIB

1 GOVT PRINTG OFC
(PDF) A MALHOTRA

25 CCDC ARL
(PDF) FCDD RLW B
C HOPPEL
FCDD RLW MB
D O'BRIEN
G GAZONAS
P MOY
T WALTER
J CLINE
FCDD RLW MA
J SANDS
E WETZEL
J LA SCALA
J TZENG
T BOGETTI
J CAIN
T PLAISTED
D SPAGNUOLO
J STANISZEWSKI
M YEAGER
C-F YEN
M NEBLETT
F RACINE
M THOMPSON
S BOYD
FCDD RLW MG
J LENHART
R MROZEK
FCDD RLW PB
S SATAPATHY
T ZHANG